Mon. Not. R. Astron. Soc. **000**, 000–000 (0000) Printed November 7, 2014 (MN LATEX style file v2.2)

On the Juno Radio Science Experiment: models, algorithms and sensitivity analysis

G. Tommei[1⋆], L. Dimare[2]†, D. Serra[1]‡, and A. Milani[1]§
[1] *Department of Mathematics, University of Pisa, Pisa, Italy*
[2] *SpaceDyS srl, Cascina (Pisa), Italy*

arXiv:1411.1613v1 [physics.space-ph] 6 Nov 2014

Accepted . Received ; in original form

ABSTRACT
Juno is a NASA mission launched in 2011 with the goal of studying Jupiter. The probe will arrive to the planet in 2016 and will be placed for one year in a polar high-eccentric orbit to study the composition of the planet, the gravity and the magnetic field. The Italian Space Agency (ASI) provided the radio science instrument KaT (Ka-Band Translator) used for the gravity experiment, which has the goal of studying the Jupiter's deep structure by mapping the planet's gravity: such instrument takes advantage of synergies with a similar tool in development for BepiColombo, the ESA cornerstone mission to Mercury. The Celestial Mechanics Group of the University of Pisa, being part of the Juno Italian team, is developing an orbit determination and parameters estimation software for processing the real data independently from NASA software ODP. This paper has a twofold goal: first, to tell about the development of this software highlighting the models used, second, to perform a sensitivity analysis on the parameters of interest to the mission.

Key words: Jupiter – radio science – gravity field – mission.

1 INTRODUCTION

The Juno mission is part of the NASA New Frontiers Program and its primary goal is the understanding of the origin and evolution of the planet Jupiter. It has been launched from Cape Canaveral on August 5, 2011 and it will complete its journey in about five years arriving to Jupiter in 2016, after having experienced an Earth fly-by in 2013.

At the end of the five year journey, the spacecraft (S/C) will be inserted in a high-eccentric polar orbit with a period of about 11 days: the perijove will be at $\sim$ 1.06 Jupiter Radii and apojove at $\sim$ 39 Jupiter Radii. The polar orbit with close perijove allows the spacecraft to avoid the bulk of the Jovian radiation field. During the nominal mission time, one year, 32 orbits will be explored and 25 of them will be dedicated to gravity science. Because of J_2 perturbation by Jupiter the latitude of perijove will change from 4 degrees to 34 degrees (see Figure 1).

Juno's activities will focus on essentially four aspects (see Matousek (2007) for more details):

- **origin**, measuring the global oxygen abundance, Juno will discriminate among different Jupiter's formation scenarios;
- **interior**, Juno will investigate the structure and convection of the Jupiter's interior and through gravity will explore the distribution of mass inside the planet;
- **atmosphere**, the mission will provide three-dimensional views of the atmosphere in order to answer to basic questions about circulation;
- **magnetosphere**, Juno will measure signatures of different auroral processes in order to study the magnetic field.

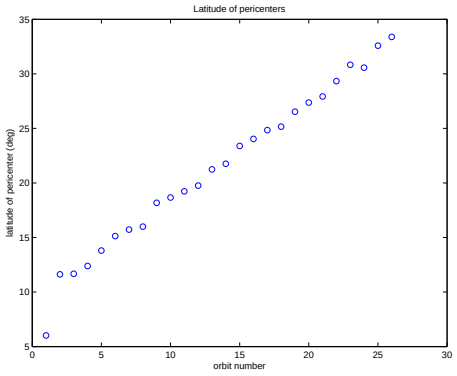

Figure 1. Perijove latitude variation during the 32 orbits of Juno.

⋆ E-mail: tommei@dm.unipi.it
† E-mail: dimare@spacedys.com
‡ E-mail: dserra@mail.dm.unipi.it
§ E-mail: milani@dm.unipi.it

The science goals of the Juno mission will be achieved with nine instruments on board the spacecraft. Among these, there is the communication subsystem to perform Doppler tracking, formed by the X-Band and Ka-Band transponders interfacing with the 34-meter Deep Space Network antenna at Goldstone, California. The Italian Space Agency (ASI) contributed to the Juno mission providing the Ka-Band Translator (KaT) (developed by the University of Rome "La Sapienza" and Thales Alenia Space) used for the gravity experiment. Such instrument takes advantage of synergies with a similar tool in development for Bepi-Colombo, the ESA cornerstone mission to Mercury (see Iess and Boscagli (2001) for more details).

The Celestial Mechanics Group of the University of Pisa is responsible for the development of an Orbit Determination (OD) and Parameters Estimation (PE) software for processing the real data independently from the NASA ones (former ODP and now MONTE); in particular, a gravimetry and a rotation experiment will be carried out by means of very accurate range-rate (doppler) observations (the accuracy should be 3×10^{-4} cm/s in range-rate, at 1000 s integration time).

Every time we have to develop a complicated software to process accurate tracking data, we have to do a preliminary work consisting in projecting the architecture of the program and in choosing the appropriate dynamical models. The aim of this paper is to describe this preliminary, but necessary, work and the description is divided in two parts essentially: in the first, we are going to describe the architecture of the software for the Juno Radio Science Experiment (RSE) and its state of the art, highlighting the theoretical models used and the problems addressed; in the second, we are going to perform a sensitivity analysis on the parameters of interest to the mission, in order to hypothesize what could be the results, in terms of parameters accuracies, of the RSE. These analysis is the basis of the future development of a differential corrector that should estimate all the interested scientific parameters.

The paper is organized as follows. In Sec. 2, we introduce fundamental definitions explaining the basics of the OD methodology used and we describe the global structure of the software pointing out the main architectural choices done in the development phase. In Sec. 3 we discuss the dynamics involved in the computation of the observables, while in Sec. 4 we underline the light-time process and the numerical methods used to avoid rounding-off errors. Sec. 5 is devoted to the sensitivity analysis of some parameters of interest and to the discussion of the results of such analysis in terms of scientific goals of the mission. In Sec. 6 we draw some conclusions and outline future developments.

2 ARCHITECTURAL STRUCTURE OF THE OD AND PE SOFTWARE FOR THE JUNO RSE

This section describes the architectural choices of the software system we are developing for the Juno RSE. The main choice done was to write a *no compromise* software. That is, no approximation, no shortcut, no choice done just to save time in the development phase, which may prove a mistake later. All approximations have been justified, that is tested and certified: this is the only way to guarantee that the results will be state of the art in all respects.

As an example, the software needs to include all the parameters which might affect the observables at the level of accuracy corresponding to the quality of the measurements (see Sec. 5). In principle, all of them could be the object of determination in a global least squares fit to the observables. Note that the design choice is to have the possibility of solving for all the unknown parameters as necessary in one step, as a global least squares fit. It is also possible to include information from other experiments by means of *a priori observations*, weighted by their normal matrix, but all the data from the RSE can be directly fit.

However, it is easy to show that some parameters which indeed affect the data are already known at a level such that they cannot be improved with the data that will be available. The simplest example is the orbit of the Moon: it certainly affects the distance between the ground station and the S/C, since the Earth moves by $\simeq 4,700$ km as a result of the motion of the Moon. Nevertheless, observing a satellite around Jupiter is certainly not a good way to constrain the orbit of the Moon: Lunar Laser Ranging (LLR) already provides the geocentric orbit of the Moon with an accuracy of few cm, thus the reflex motion of the Earth around the Earth-Moon barycenter to better than 1 mm. A similar argument applies to the satellites of Jupiter: the satellites, especially the four Galilean ones, have a significant effect on the orbit of Juno, still the uncertainty in these perturbations is small. The Juno S/C will in fact neither accurately measure the positions of the satellites nor pass close enough to them to be able to measure their gravitational attraction with useful accuracy. This implies that some of the parameters, including those contained in the ephemerides of the Moon and other planets, in the rotation state of the Earth, in the ephemerides of Jupiter's satellites, and others, do appear in the observables but have to be handled as *consider parameters*, not to be determined, after checking that their present uncertainty is such that their contribution to the uncertainty of the observable is negligible.

2.1 OD background

From the algorithmic point of view, the software consists in a non linear least square differential correction fit of the doppler tracking data in order to determine the following quantities, generally referred to as $\mathbf{u}$:

1) initial conditions of the S/C at given times;
2) spherical harmonics of the gravity field of Jupiter according to following potential (R is the radius of Jupiter)

$$U(r,\theta,\lambda) = \frac{GM}{r}\sum_{\ell=0}^{+\infty}\sum_{m=0}^{\ell}\frac{R^\ell}{r^\ell}[C_{\ell m}\cos(m\lambda) + S_{\ell m}\sin(m\lambda)]P_{\ell m}(\sin\theta) \ ;$$

3) Love's number for the tidal deformation of Jupiter (static tidal theory), according to the following potential

$$U_{\text{Love}} = \sum_{\ell=2}^{+\infty} k_\ell \frac{GM_P R^{2\ell+1}}{r_P^{\ell+1} r^{\ell+1}} P_\ell(\cos\varphi) \ ;$$

4) parameters defining the model of the Jupiter's rotation;

5) the angular momentum of Jupiter through the Lense-Thirring (LT) effect causing an acceleration

$$\mathbf{a}_{LT} = \frac{2\,G}{c^2\,r^3}\left[-\mathbf{J}\times\dot{\mathbf{r}} + 3\,\frac{(\mathbf{J}\cdot\mathbf{r})\,(\mathbf{r}\times\dot{\mathbf{r}})}{r^2}\right] ;$$

5) initial conditions for the Barycenter of the Jovian System (BJS) at some initial time;
6) relativistic Post-Newtonian Parameter (PPN) γ during the Superior Conjuction Experiment (SCE).

Of course a good initial guess for each of the above parameters will be also necessary: the navigation team should supply the initial conditions of the S/C, the gravity and physical parameters will be taken by previous investigations, the initial conditions for BJS will be provided by JPL Ephemerides DE421 (see Folkner et al. (2008)) and for γ will be used the General Relativity (GR) value 1.

Following a classical approach (see, for instance, Milani and Gronchi (2010)), the non linear least squares fit aims at computing a set of parameters $\mathbf{u}^*$ which minimizes the target function:

$$Q(\mathbf{u}) = \frac{1}{m}\boldsymbol{\xi}^T(\mathbf{u})W\boldsymbol{\xi}(\mathbf{u}) = \frac{1}{m}\sum_{i=1}^{m} w_i\xi_i^2(\mathbf{u}), \qquad (1)$$

where m is the number of observations and $\boldsymbol{\xi} = \mathcal{O}-\mathcal{C}$ is the vector of *residuals*, difference between the observed quantities $\mathcal{O}$ and the predicted ones $\mathcal{C}(\mathbf{u})$, computed following suitable models and assumptions (described in the next sections). $\mathcal{O}$ are range and/or range-rate data, while $\mathcal{C}(\mathbf{u})$ are the results of the light-time computations (see Sec. 4 and Tommei et al. (2010)) as a function of all the quantities $\mathbf{u}$ listed above. Finally, w_i is the weight associated to the $i-$observation.

Among the parameters $\mathbf{u}$, 1), 2) and 3) are present in the equations of motion for the jovicentric orbit of the spacecraft, while 4) and 5) in those for the barycentric orbit of BJS (see Sec. 3).

Other information required to such orbit propagations are supposed to be known: position and velocity for the other planets of the Solar System are obtained from the JPL ephemerides DE421; the rotation of the Earth is provided by the interpolation table made public by the International Earth Rotation Service (IERS) and the coordinates associated with the ground stations are expected to be available.

The procedure to compute $\mathbf{u}^*$ is based on a modified Newton's method known in the literature as *differential corrections method*. Let us define

$$B = \frac{\partial\boldsymbol{\xi}}{\partial\mathbf{u}}(\mathbf{u}), \qquad C = B^T W B,$$

which are called the *design* matrix and the *normal* matrix, respectively. Then the correction:

$$\Delta\mathbf{u} = C^{-1}D \quad \text{with } D = -B^T W\boldsymbol{\xi} \qquad (2)$$

is applied iteratively until either Q does not change meaningfully from one iteration to the other or $\Delta\mathbf{u}$ becomes smaller than a given tolerance.

2.2 Simulators and correctors

The structure of the overall software is outlined in Fig. 2. In general, developing a software for OD and PE, the main

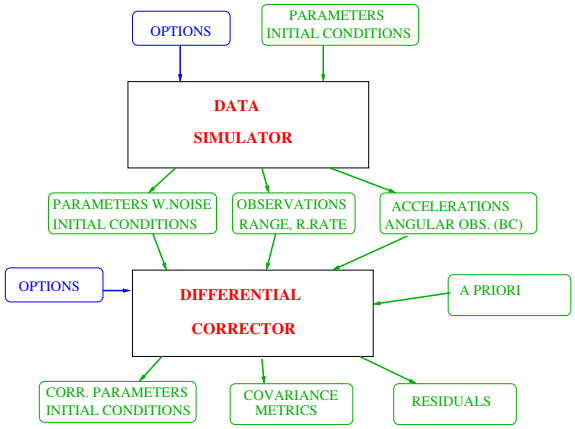

Figure 2. The block diagram of a simple simulator setup. The black rectagles indicate the main programs, the rectangles with smoothed corners the data structures.

programs belong to two categories: **data simulators** (short: simulators) and **differential correctors** (short: correctors). The simulators generate simulated observables (range and range-rate, accelerations) and preliminary orbital elements. The correctors solve for all the parameters which can be determined by a least squares fit (possibly constrained and/or decomposed in a multi-arc structure). The simulators have a fundamental role because the real data are available many years in the future, while in the present we have the necessity of studying the possibility to estimate some parameters in order to achieve the scientific goals.

The program structure of the simulator is comparatively simple, with all the complexity in the dynamics (Sec. 3), observations (Sec. 4) and error models. The corrector structure has to be designed in a very careful way. One of the goals of our software development is to be able to exploit parallel computing, especially for the most computationally expensive portion of the processing. The propagation of the jovicentric orbit contains most of the computational complexity, together with the light-time computation. Thus the idea is to parallelize the computation of the jovicentric dynamics and of the observables, with the relative partial derivatives, and also the composition of the design matrix, the normal matrix, and the inversion of the local normal matrices.

The choice of the method for the estimation of parameters, following what we have done for the similar software for the BepiColombo RSE (see, for example, Alessi et al. (2012)), should be essentially twofold:

- **multi-arc strategy**: according to this method, every single arc has its own set of initial conditions; in this way, the actual errors in the orbit propagation, due to lack of knowledge in the non-gravitational dynamical model, can be reduced by an over-parametrization of the initial conditions;
- **constrained multi-arc strategy**: this method is established on the idea that each observed arc belongs to the same object (the S/C) and thus the orbits corresponding to two subsequent extended arcs (we call "extended arc" an observed arc broadened out from half of the dark period before it to half of the dark period after it) should coincide at the connection time in the middle of the non-observed interval.

In the development of the corrector we are going to investigate both approaches, even if we are quite convinced that the multi-arc approach will be the right way.

2.3 Propagators and multiple dynamics

The observables depend on multiple dynamics, thus the main programs need to have available the propagated state for each dynamics (for the list of dynamics, see Sec. 3). This is obtained in different ways, depending upon the dynamics.

- For the dynamics which have to be propagated by numerical integration that is the S/C around Jupiter, the Barycenter of Jovian System orbit, and the S/C interplanetary orbit we call a propagator which uses the corresponding dynamic module and solves the equation of motion, for the requested time interval. The states (time, position, velocity, acceleration) are stored in a memory stack, from which interpolation is possible with the required accuracy. Then, when the state is needed to compute the observables, the dynamics stacks are consulted and interpolated by the propagator modules.
- The dynamics of the Jupiter rotation is represented by a semi-empirical model and the state is computed as an explicit function of time.
- For the dynamics of the Earth rotation, for which an interpolation table is already available from an external source (IERS), the interpolation is performed inside the corresponding dynamical module.
- For the planetary ephemerides and the Jupiter's satellites ephemerides the interpolation tables are provided from JPL, together with the interpolation software which has been adapted for the insertion in our code. The time ephemerides, to convert between different time systems, are not currently available from JPL and therefore they are propagated in a suitable dynamics.

There could be more than one propagator module, in particular because of the need of quadruple precision computations for the heliocentric orbits. However, the architecture is compatible with M propagators/interpolators acting on N dynamics.

3 DYNAMICS

In this section, for the case of Juno around Jupiter, the dynamics which affect the observables are described. For the SCE, thinked to constrain the PN parameter γ, a separate software has been implemented, but it will not be described in this paper: for more details, see Tommei et al. (2012).

3.1 Time ephemerides

The time coordinate which must be used for the formulation of the full relativistic equations of motion for an orbiter around a planet (Damour at al. (1994)) is the dynamical time relative to the planet, essentially the proper time of a body moving with the center of mass of the planet (Tommei et al. (2010)). For Jupiter we need to define a Jupiter Dynamical Time (TDJ) containing terms of 1-PN order depending mostly upon the distance r_0 from the Sun and velocity v of Jupiter. The relationship with the TDB scale,

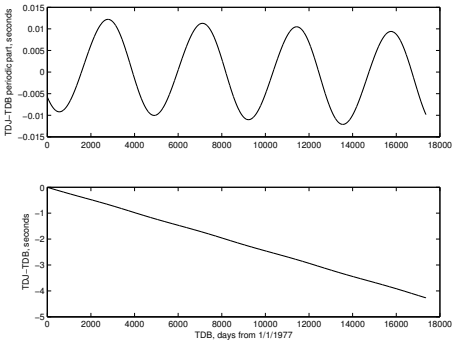

Figure 3. Top: the oscillatory term, with the period of Jupiter's orbit. Bottom: Linear drift with respect to TDB.

truncated to 1-PN order (we drop the $O(c^{-4})$ terms on the right hand side, that are in principle known, but certainly not needed for our purposes), is given by a differential equation

$$\frac{dt_{\rm TDJ}}{dt_{\rm TDB}} = 1 - \frac{v^2}{2\,c^2} - \sum_{k \neq jup} \frac{G\,m_k}{c^2\,r_k} \ ,$$

which can be solved by a quadrature formula once the orbits of Mercury, the Sun and the other planets are known. Figure 3 plots the output of such a computation, showing a drift due to the non-zero average of the post-Newtonian term.

The dynamical times relative to the planets, including the one relative to the Earth, Terrestrial Dynamical Time (TDT, also shortly indicated as TT) are defined as a function of the Barycentric Dynamical Time (TDB) by the same separable differential equation. In our software We use a Gaussian quadrature formula to generate an interpolation table for the conversion from TDB to TDT, TDJ. This table is precomputed by a separate main program and it can be read by all other programs: a suitable module uses the interpolation to compute all conversions of time coordinates, that is it implements an internal system of time ephemerides.

3.2 S/C around Jupiter

The orbit of Juno, when already in orbit around Jupiter, has an equation of motion containing:

- the spherical harmonics of the gravity field of Jupiter,
- the non gravitational perturbations, including direct radiation pressure, pressure from radiation reflected and emitted by Jupiter, thermal emission;
- solar and planetary differential attractions and tidal perturbations,
- Jupiter's satellite differential attractions and tidal perturbations,
- relativistic corrections.

There are two main relativistic corrections in the jovicentric orbit: one is due to the need to use proper time TDJ affected by the gravitational potential at the center of mass of Jupiter; the second is the Lense-Thirring (LT) effect depending upon the angular momentum of Jupiter.

3.3 Orbit of BJS

The orbit of the BJS, centered at the Solar System Barycenter (SSB) has an equation of motion (computed in TDB) including:

- the Newtonian attraction from the Sun and the planets;
- the relativistic PPN corrections, including the PN parameters γ, β and the Sun's dynamic oblateness;
- the effects of possible violations of GR are limited to possible changes to the parameter γ, which shall be tested in a SCE in the cruise phase;
- the effect of the satellites on the motion of the BJS.

The decomposition of the motion of Jupiter into the sum of two state vectors, the BJS centered at the SSB and Jupiter centered at the BJS, is classical in Newtonian mechanics (Jacobian vectors) but far from trivial in a full relativistic PPN formalism. Thus for the BJS the attractions listed above need to be computed as the resultant attraction on Jupiter and on the major satellites, but there may be additional relativistic terms which are relevant.

The effect of the satellites on the orbit of the BJS is small (Roy-Walker smallness parameter 1.5×10^{-10}), but large enough to affect the residuals of the RSE at a level above the noise.

3.4 Rotation of Jupiter and of the Earth

For the rotation of Jupiter we use a semi-empirical model, containing parameters defining the model of the Jupiter's rotation, essentially two angles δ_1 and δ_2 specifying the direction of the rotation axis with respect to the direction given by the IAU (Archinal et al. (2011)).

For the Earth we are using the interpolation tables made public by the International Earth Rotation Service (IERS), because there is no way to solve for Earth rotation parameters from observations at Jupiter (at accuracies competitive with other available measurements),

The same argument applies to the station coordinates, which we have to assume are supplied by the ground station with the required accuracy, including corrections for the antenna motion.

3.5 Planetary ephemerides

The current state, as a function of time, of the planets Mercury to Neptune (excluding Jupiter and considering also Pluto) are read from the JPL ephemerides (currently the DE421 version, Folkner et al. (2008)) as Chebichev polynomials, which are interpolated with the JPL well tested algorithm. For Jupiter satellites the ephemerides are provided by JPL in the form of SPICE kernels (Jacobson (2003)): the SPICE software has been linked and suitable interfaces have been implemented in the code. These ephemerides use the TDB time coordinate.

We need also to take into account asteroid perturbations on the orbit of the BJS. The software to generate asteroid ephemerides interpolation tables is available, and the interface has been built, to be used with as many asteroids as needed. At the moment, for consistency with DE421 we use the perturbations from 343 asteroids, each one with a mass as assigned by the ephemerides.

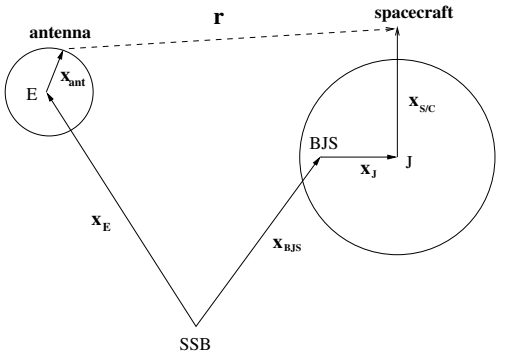

Figure 4. Geometric sketch of the vectors involved in the computation of the range. SSB is the Solar System Barycenter, J is the center of Jupiter, BJS is the barycenter of the jovian system, E is the center of the Earth.

4 OBSERVABLES

As it is well clear in space navigation (see, for instance, Moyer (2003)), the distance to a spacecraft cannot be computed by an explicit analytic formula from the state of the ground station and the spacecraft at the same time, but we need some *light-time iterations*. In the Juno case the equation giving the range (distance antenna-spacecraft, equivalent to the light-time up to a factor c, see Fig.4) is

$$r = |(\mathbf{x}_{S/C} + \mathbf{x}_{BJS} + \mathbf{x}_J) - (\mathbf{x}_E + \mathbf{x}_{ant})| + S(\gamma) \qquad (3)$$

where $\mathbf{x}_{S/C}$ is the jovicentric position of the orbiter, $\mathbf{x}_{BJS}$ is the position of the center of mass of Jupiter's system in a reference system with origin at SSB, $\mathbf{x}_J$ is the vector from the BJS to the center of mass of Jupiter, $\mathbf{x}_E$ is the position of the Earth center of mass with respect to SSB, $\mathbf{x}_{ant}$ is the position of the reference point of the ground antenna with respect to the center of mass of the Earth, and $S(\gamma)$ is the *Shapiro effect*.

Using (3) means to model the space as a flat arena (r is an Euclidean distance) and the time as an absolute parameter. This is obviously not possible because it is clear that, beyond some threshold of accuracy, space and time have to be formulated within the framework of Einstein's theory of gravity (GR). Moreover we have to take into account the different times at which the events have to be computed: the transmission of the signal at the transmit time (t_t), the signal at the Jupiter orbiter at the time of bounce (t_b) and the reception of the signal at the receive time (t_r). Formula (3) is used as a starting point to construct a correct relativistic formulation; with the word "correct" we do not mean all the possible relativistic effects, but the effects that can be measured by the experiment.

The five vectors involved in formula (3) have to be computed at their own time, the epoch of different events: e.g., $\mathbf{x}_{\rm ant}$ and $\mathbf{x}_{\rm E}$ are computed at both the antenna *transmit time* t_t and *receive time* t_r of the signal, $\mathbf{x}_{\rm S/C}$, $\mathbf{x}_{\rm BJS}$ and $\mathbf{x}_{\rm J}$ are computed at the *bounce time* t_b (when the signal has arrived to the orbiter and is sent back, with correction for the delay of the transponder). In order to be able to perform the vector sums and differences, these vectors have to be converted to a common space-time reference system, the only possible choice being some realization of the BCRS (Barycentric Celestial Reference System). We adopt for now a realization of the BCRS that we call SSB reference frame and in which

the time is a re-definition of the TDB; other possible choices, such as TCB (Barycentric Coordinate Time), only can differ by linear scaling. The TDB choice of the SSB time scale entails also the appropriate linear scaling of space-coordinates and planetary masses as described for instance in Klioner et al. (2010).

The vectors $\mathbf{x}_{\rm BJS}$ and $\mathbf{x}_{\rm E}$ are already in SSB as provided by numerical integration and external ephemerides; thus the vectors $\mathbf{x}_{\rm ant}$, $\mathbf{x}_{\rm J}$ and $\mathbf{x}_{\rm S/C}$ have to be converted to SSB from the geocentric and jovicentric systems, respectively. Of course the conversion of reference system implies also the conversion of the time coordinate. There are three different time coordinates to be considered. The currently published planetary ephemerides are provided in TDB. The observations are based on averages of clock and frequency measurements on the Earth surface and the time coordinate is TT. Thus for each observation the times of transmission t_t and reception t_r need to be converted from TT to TDB to find the corresponding positions of the planets by combining information from the pre-computed ephemerides and the output of the numerical integration for the BJS. This time conversion step is necessary for the accurate processing of each set of interplanetary tracking data; the main term in the difference TT-TDB is periodic, with period 1 year and amplitude $\simeq 1.6 \times 10^{-3}$ s, while there is essentially no linear trend, as a result of a suitable definition of the TDB.

From now on, in accordance with Klioner et al. (2010), we shall call the quantities related to the SSB frame "TDB-compatible", the quantities related to the geocentric frame "TT-compatible", the quantities related to the jovicentric frame "TDJ-compatible" and label them TB, TT and TJ, respectively.

The differential equation giving the local time T as a function of the SSB time t , which we are currently assuming to be TDB, is the following:

$$\frac{dT}{dt} = 1 - \frac{1}{c^2}\left[U + \frac{v^2}{2} - L\right] , \qquad (4)$$

where U is the gravitational potential (the list of contributing bodies depends upon the accuracy required: in our implementation we use Sun, Mercury to Neptune, Moon) at the planet center and v is the SSB velocity of the same planet. The constant term L is used to perform the conventional rescaling motivated by removal of secular terms.

The space-time transformations to perform involve essentially the position of the antenna and the position of the orbiter. The geocentric coordinates of the antenna should be transformed into TDB-compatible coordinates; the transformation is expressed by the formula

$$\mathbf{x}^{TB}_{\rm ant} = \mathbf{x}^{TT}_{\rm ant}\left(1 - \frac{U}{c^2} - L_C\right) - \frac{1}{2}\left(\frac{\mathbf{v}^{TB}_{\rm E}\cdot\mathbf{x}^{TT}_{\rm ant}}{c^2}\right)\mathbf{v}^{TB}_{\rm E} ,$$

where U is the gravitational potential at the geocenter (excluding the Earth mass), $L_C = 1.48082686741 \times 10^{-8}$ is a scaling factor given as definition, supposed to be a good approximation for removing secular terms from the transformation and $\mathbf{v}^{TB}_{\rm E}$ is the barycentric velocity of the Earth. The next formula contains the effect on the velocities of the time coordinate change, which should be consistently used together with the coordinate change:

$$\mathbf{v}^{TB}_{\rm ant} = \left[\mathbf{v}^{TT}_{\rm ant}\left(1 - \frac{U}{c^2} - L_C\right) - \frac{1}{2}\left(\frac{\mathbf{v}^{TB}_{\rm E}\cdot\mathbf{v}^{TT}_{\rm ant}}{c^2}\right)\mathbf{v}^{TB}_{\rm E}\right]\left[\frac{dT}{dt}\right] .$$

Note that the previous formula contains the factor dT/dt (expressed by (4)) that deals with a time transformation: T is the local time for Earth, that is TT, and t is the corresponding TDB time.

The jovicentric coordinates of the orbiter have to be transformed into TDB-compatible coordinates through the formula

$$\mathbf{x}^{TB}_{\rm S/C} = \mathbf{x}^{TJ}_{\rm S/C}\left(1 - \frac{U}{c^2} - L_{CJ}\right) - \frac{1}{2}\left(\frac{\mathbf{v}^{TB}_{\rm M}\cdot\mathbf{x}^{TJ}_{\rm S/C}}{c^2}\right)\mathbf{v}^{TB}_{\rm M} ,$$

where U is the gravitational potential at the center of mass of Jupiter (excluding the Jupiter mass) and L_{CJ} could be used to remove the secular term in the time transformation (thus defining a TJ scale, implying a rescaling of the mass of Jupiter). We believe this is not necessary: the secular drift of TDJ with respect to other time scales is significant, but a simple iterative scheme is very efficient in providing the inverse time transformation. Thus we set $L_{CJ} = 0$, assuming the reference frame is TDJ-compatible. As for the antenna we have a formula expressing the velocity transformation that contains the derivative of time T for Jupiter, that is TDJ, with respect to time t, that is TDB:

$$\mathbf{v}^{TB}_{\rm S/C} = \left[\mathbf{v}^{TJ}_{\rm S/C}\left(1 - \frac{U}{c^2} - L_{CJ}\right) - \frac{1}{2}\left(\frac{\mathbf{v}^{TB}_{\rm M}\cdot\mathbf{v}^{TJ}_{\rm S/C}}{c^2}\right)\mathbf{v}^{TB}_{\rm M}\right]\cdot\left[\frac{dT}{dt}\right]$$

For these coordinate changes, in every formula we neglected the terms of the SSB acceleration of the planet center, because they contain beside $1/c^2$ the additional small parameter (distance from planet center)/(planet distance to the Sun), which is of the order of 10^{-4}.

The correct modeling of space-time transformations is not sufficient to have a precise computation of the signal delay: we have to take into account the general relativistic contribution to the time delay due to the space-time curvature under the effect of the Sun's gravitational field (or Jupiter gravitational field), the *Shapiro effect* Shapiro (1964). The Shapiro time delay Δt at the 1-PN level, according to Moyer (2003), is

$$\Delta t = \frac{(1+\gamma)\,\mu_0}{c^3}\,\ln\left(\frac{r_t + r_r + r}{r_t + r_r - r}\right) , \quad S(\gamma) = c\,\Delta t$$

where $r_t = |\mathbf{r}_{\rm t}|$ and $r_r = |\mathbf{r}_{\rm r}|$ are the heliocentric distances of the transmitter and the receiver at the corresponding time instants of photon transmission and reception, μ_0 is the gravitational mass of the Sun (or Jupiter) and $r = |\mathbf{r}_r - \mathbf{r}_t|$. Parameter γ is the only post-Newtonian parameter used for the light-time effect and, in fact, it could be best constrained during superior conjunction. The question arises whether the very high signal to noise in the range requires other terms in the solar gravity influence, due to higher-order corrections when the radio waves are passing near the Sun, at just a few solar radii (and thus the denominator in the log-function of the Shapiro formula is small). These corrections are of order 2, (containing a factor $1/c^4$): the relevant correction is most easily obtained by adding $1/c^4$ terms in the Shapiro formula, due to the bending of the light path:

$$S(\gamma) = \frac{(1+\gamma)\,\mu_0}{c^2}\,\ln\left(\frac{r_t + r_r + r + \frac{(1+\gamma)\,\mu_0}{c^2}}{r_t + r_r - r + \frac{(1+\gamma)\,\mu_0}{c^2}}\right) .$$

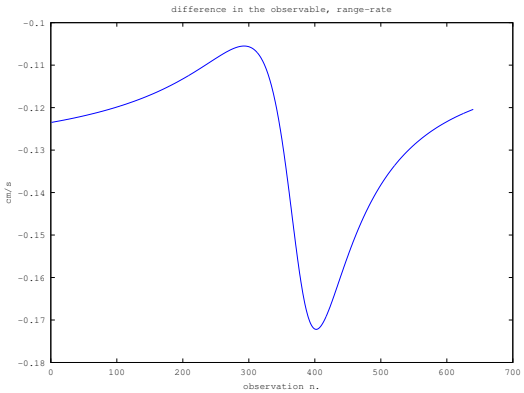

Figure 5. Total amount of the Shapiro effect, both for the Sun and Jupiter, in range-rate observable over 2-year simulation.

This formulation has been proposed by Moyer (2003) and it has been justified in the small impact parameter regime by much more theoretically rooted derivations by other authors. The total amount of the Shapiro effect in range-rate is shown in Figure 5: see Tommei et al. (2010) for a detailed description of the Shapiro delay for the range-rate observable.

Of course, the light-time computation is an iterative procedure. In particular, since radar measurements are usually referred to the receive time t_r, the observables are seen as functions of this time, and the computation sequence works backward in time: starting from t_r, the bounce time t_b is computed iteratively (down-leg iterations), and, using this information the transmit time t_t is computed (up-leg iterations).

4.1 Integrated observables

A problem well known to radio science experts is that for top accuracy the range-rate measurement cannot be the instantaneous value (up: up-leg, do: down-leg)

$$\dot{r}(t_r) = (\dot{r}_{up}(t_r) + \dot{r}_{do}(t_r))/2 \ .$$

In fact, the measurement is not instantaneous: an accurate measure of a Doppler effect requires to fit the difference of phase between carrier waves, the one generated at the station and the one returned from space, accumulated over some *integration time* Δ, typically between 10 and 1000 s. Thus the observable is really a difference of ranges

$$r(t_b + \Delta/2) - r(t_b - \Delta/2) = \int_{t_b-\Delta/2}^{t_b+\Delta/2} \dot{r}(s)\ ds$$

or, equivalently, an averaged value of range-rate over the integration interval

$$\dot{r}_\Delta(t_r) = \frac{1}{\Delta} \int_{t_b-\Delta/2}^{t_b+\Delta/2} \dot{r}(s)\ ds \ . \qquad (5)$$

We decided to implement a quadrature formula to approximate the integral of eq. (5) because it allows to control much better the rounding off problems, because the relative accuracy in range-rate is by no means as extreme as the one required to implement the $r(t_b + \Delta/2) - r(t_b - \Delta/2)$ computation. In Milani et al. (2010) some figures describing this issue are present.

5 SENSITIVITY ANALYSIS

In this section we want to discuss some results concerning the scientific goals of the mission obtained with simulated data and running *sensitivity tests*. This kind of tests consists in varying of some extent the default value of a parameter and to see if the observable is affected, in the limit of the accuracy, by such variation. But the first thing to do is to compile a list of all the effects, both dynamical (that is acting on the orbit) and observational (that is acting on the light-time and its time derivative) that can change the motion of the spacecraft in orbit around Jupiter and then modify the observable down to the observational noise level. The major dynamical effects are described in Tab. 1: the table contains the effect (e.g. the Lense-Thirring effect), its formulation and its value in cm/s^2.

We can note that, a part from the gravitational field of Jupiter, the strongest perturbation is the gravitational one of the Io satellite, while the gravitational perturbations from Europa and Ganymede are of the same order of the solid tides due to Io and the relativistic perturbation of Jupiter. It is clear from the table that the inclusion of Galilean satellites in the model is necessary, but, in our investigations, we also found that the satellites Amalthea and Thebe play an important role, as we will show in Subsec. 5.1. At the moment we are not taking into account non-gravitational effects, although we are aware that to get a good determination of the parameters of interest it will be necessary to estimate these effects.

In the next subsections we are going to display some figures showing the changes in the observable range and range-rate, even if, for the Juno mission, only the doppler data, corresponding to range rate, will be available for accurate radio science experiments. We want to stress that this preliminary work is necessary but not sufficient to know if a parameter estimation will experience a success, there a lot of sources of error that could be taken into account, but this aspect will be the subject of a next paper.

5.1 Satellites and solid tides

As mentioned before, the role of the Galilean satellites is fundamental, but also Amalthea and Thebe affects the observables. In Fig. 6 we show the sensitivity of the Juno observables (above range, below range-rate) to the perturbations from Amalthea and Thebe, over an arc centered at perijove supposing a noise from KAT at $\simeq 3 \times 10^{-4}$ cm/s for an integration time of 1000 seconds. The figure is obtained as difference between a run of the software including in the model Amalthea and Thebe and a run with only the Galilean satellites. The Signal-to-Noise (S/N) ratio is, for the range-rate, about 50, that is the signal from the two satellites is distinguishable and we could try to improve our understanding on this two satellites.

From Tab. 1 it is clear how important it is to take into account the solid tides, not only due to the Sun but also those resulting from the Galilean satellites: the next three figures show how different degrees, described using the Love numbers k_j as parameters to be determined, affect the observables.

Fig. 7 represents the perturbations from the tidal degree

Cause	Formula	Parameters	Value cm/s^2
Jupiter monopole	$GM_{jup}/r^2 = F_0$	GM_{jup}	2.3×10^3
Jupiter oblateness	$3\,F_0\,\overline{C}_{20}\,R_{jup}^2/r^2$	$\overline{C}_{20}$	1.2×10^2
Jupiter C_{40}	$5\,F_0\,\overline{C}_{40}\,R_{jup}^4/r^4$	$\overline{C}_{40}$	5.0
Jupiter C_{60}	$7\,F_0\,\overline{C}_{60}\,R_{jup}^6/r^6$	$\overline{C}_{60}$	-3.54×10^{-1}
Jupiter C_{30}	$4\,F_0\,\overline{C}_{30}\,R_{jup}^3/r^3$	$\overline{C}_{30}$	4.7×10^{-3}
Jupiter S_{22}	$3\,F_0\,\overline{S}_{22}\,R_{jup}^2/r^2$	$\overline{S}_{22}$	-7.6×10^{-5}
Jupiter triaxiality	$3\,F_0\,\overline{C}_{22}\,R_{jup}^2/r^2$	$\overline{C}_{22}$	3.52×10^{-5}
Io pert.	$2\,GM_{io}\,r/r_{j\,io}^3$	GM_{io}	1.2×10^{-3}
Europa pert.	$2\,GM_{eur}\,r/r_{j\,e}^3$	GM_{eur}	1.6×10^{-4}
Ganymede pert.	$2\,GM_{gan}\,r/r_{j\,g}^3$	GM_{gan}	1.2×10^{-4}
Relativistic Jupiter	$F_0\,4\,G\,M_{jup}/(c^2\,r)$	$G\,M_{jup}$	1.7×10^{-4}
Solid tide (Io)	$3k_2\,GM_{io}\,R_{jup}^5/(r_{J\,io}^3\,r^4)$	k_2	8.9×10^{-4}
Solid tide (Europa)	$3k_2\,GM_{eur}\,R_{jup}^5/(r_{J\,eur}^3\,r^4)$	k_2	1.2×10^{-4}
Solid tide (Io)	$4k_3\,GM_{io}\,R_{jup}^7/(r_{J\,io}^4\,r^5)$	k_3	1.8×10^{-4}
Solid tide (Ganymede)	$3k_2\,GM_{gan}\,R_{jup}^5/(r_{J\,gan}^3\,r^4)$	k_2	8.2×10^{-5}
Solid tide (Io)	$5k_4\,GM_{io}\,R_{jup}^9/(r_{J\,io}^5\,r^6)$	k_4	3.6×10^{-5}
Lense-Thir.	$6\,GJ_{jup}\lvert\dot{\mathbf{r}}\rvert/c^2\,r^3$	GJ_{jup}	2.5×10^{-5}
Callisto pert.	$2\,GM_{cal}\,r/r_{j\,c}^3$	GM_{cal}	1.6×10^{-5}
Solid tide (Europa)	$4k_3\,GM_{eur}\,R_{jup}^7/(r_{J\,eur}^4\,r^5)$	k_3	1.5×10^{-5}
Solid tide (Callisto)	$3k_2\,GM_{cal}\,R_{jup}^5/(r_{J\,cal}^3\,r^4)$	k_2	1.2×10^{-5}
Solid tide (Ganymede)	$4k_3\,GM_{gan}\,R_{jup}^7/(r_{J\,gan}^4\,r^5)$	k_3	6.5×10^{-6}
Sun pert.	$2\,GM_{\odot}\,r/r_{\odot}^3$	$GM_{\odot}$	4.7×10^{-6}
Solid tide (Sun)	$3k_2\,GM_{\odot}\,R_{jup}^5/(r_{J\,\odot}^3\,r^4)$	k_2	3.1×10^{-6}
Solid tide (Europa)	$5k_4\,GM_{eur}\,R_{jup}^9/(r_{J\,eur}^5\,r^6)$	k_4	1.9×10^{-6}
Solid tide (Callisto)	$4k_3\,GM_{cal}\,R_{jup}^7/(r_{J\,cal}^4\,r^5)$	k_3	5.3×10^{-7}
Solid tide (Ganymede)	$5k_4\,GM_{gan}\,R_{jup}^9/(r_{J\,gan}^5\,r^6)$	k_4	4.8×10^{-7}
Amalthea pert.	$2\,GM_{ama}\,r/r_{J\,ama}^3$	GM_{ama}	3.5×10^{-7}
Solid tide (Amalthea)	$3k_2\,GM_{ama}\,R_{jup}^5/(r_{J\,ama}^3\,r^4)$	k_2	2.6×10^{-7}
Thebe pert.	$2\,GM_{the}\,r/r_{J\,the}^3$	GM_{the}	1.4×10^{-7}
Solid tide (Amalthea)	$4k_3\,GM_{ama}\,R_{jup}^7/(r_{J\,ama}^4\,r^5)$	k_3	1.2×10^{-7}
Solid tide (Thebe)	$3k_2\,GM_{the}\,R_{jup}^5/(r_{J\,the}^3\,r^4)$	k_2	1.0×10^{-7}
Solid tide (Amalthea)	$5k_4\,GM_{ama}\,R_{jup}^9/(r_{J\,ama}^5\,r^6)$	k_4	5.5×10^{-8}
Solid tide (Thebe)	$4k_3\,GM_{the}\,R_{jup}^7/(r_{J\,the}^4\,r^5)$	k_3	4.0×10^{-8}
Solid tide (Callisto)	$5k_4\,GM_{cal}\,R_{jup}^9/(r_{J\,cal}^5\,r^6)$	k_4	2.3×10^{-8}
Solid tide (Thebe)	$5k_4\,GM_{the}\,R_{jup}^9/(r_{J\,the}^5\,r^6)$	k_4	1.5×10^{-8}
Solid tide (Sun)	$4k_3\,GM_{\odot}\,R_{jup}^7/(r_{J\,\odot}^4\,r^5)$	k_3	3.4×10^{-10}
Solid tide (Sun)	$5k_4\,GM_{\odot}\,R_{jup}^9/(r_{J\,\odot}^5\,r^6)$	k_4	3.6×10^{-14}

Table 1. Accelerations acting on a spacecraft in orbit around Jupiter, in a planetocentric reference frame, with $r = 75000$ km.

2 term from all the Galilean satellites and the Sun, acting together with a frequency-independent k_2 (for the simulation $k_2 = 0.7$ has been assumed) and it points out that the parameter k_2 could be determined very well ($S/N \simeq 2000$).

Fig. 8 shows the sensitivity of the observables to the tidal degree 3 term from all the Galilean satellites and the Sun, acting together with a frequency-independent k_3 (for the simulation $k_3 = 0.7$ has been assumed): the S/N is about 300 and it means that we could extract information about k_3 from the data.

Going on with the exploration of the higher degrees of the solid tide we arrive to Fig. 9, where the sensitivity of the observables to the tidal degree 4 term from all the Galilean satellites and the Sun is shown (for the simulation $k_4 = 0.7$ has been assumed): the S/N is about 20 and it means that we could extract information from the data also about k_4.

5.2 Relativistic effects

The Juno mission has not been designed to improve the knowledge about GR: a SCE, with the goal of constraining the parameter γ has been performed last summer, but it is fairly certain that the results cannot improve that obtained with the Cassini mission (Bertotti et al. (2003)). However, the S/C is exposed to significant relativistic effects. In particular, the high velocity at pericenter (60 km/s), in combination with Jupiter's fast rotation ($T =$ 10 h), induces a significant acceleration due to the Lense-Thirring (LT) precession. In the low-velocity, weak field approximation, this acceleration is proportional to the angular momentum of the central body and to the velocity of the test particle, and orthogonal to them. A measurement of the LT precession would therefore provide also the angular momentum of the planet. As the perturbing field rapidly decreases with the radial distance, by far the largest acceleration occurs during the pericenter pass (about 6 h). This unique opportunity to

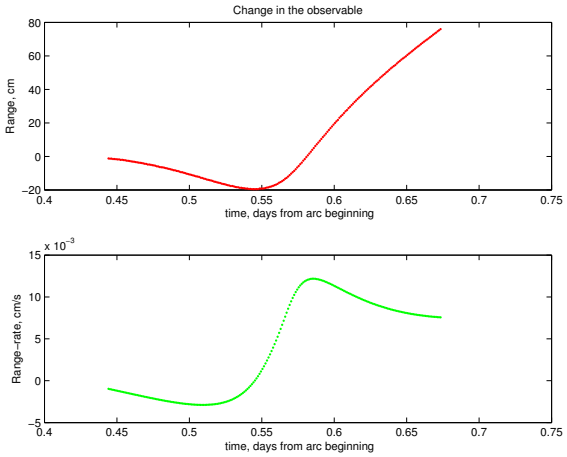

Figure 6. Perturbations from Amalthea and Thebe.

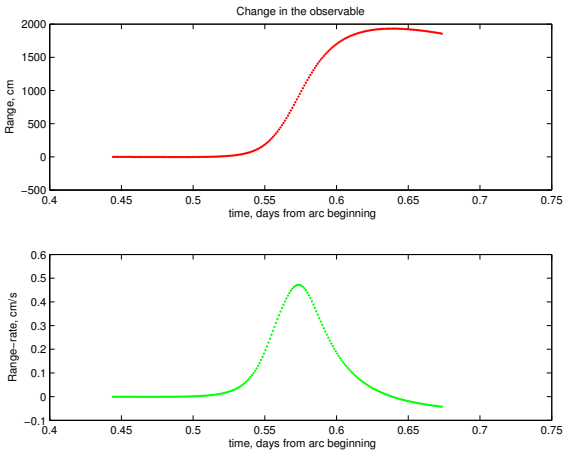

Figure 7. Perturbations from the tidal degree 2 term from all the Galilean satellites and the Sun.

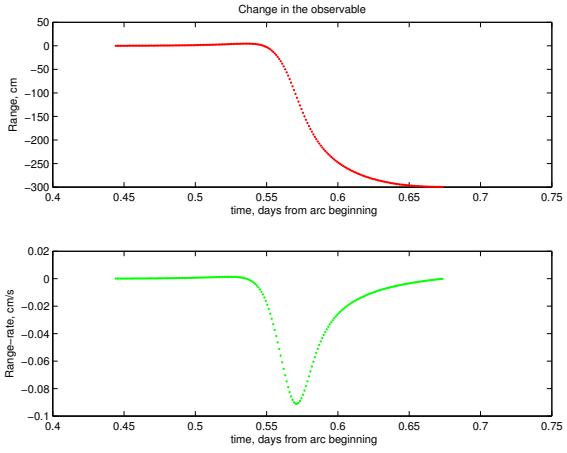

Figure 8. Perturbation from the tidal degree 3 term from all the Galilean satellites and the Sun.

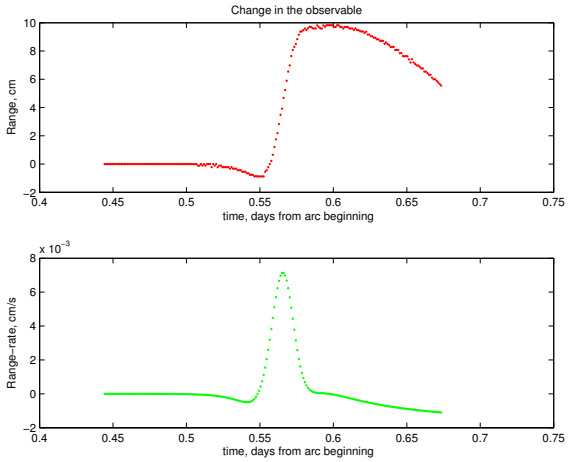

Figure 9. Perturbation from the tidal degree 4 term from all the Galilean satellites and the Sun.

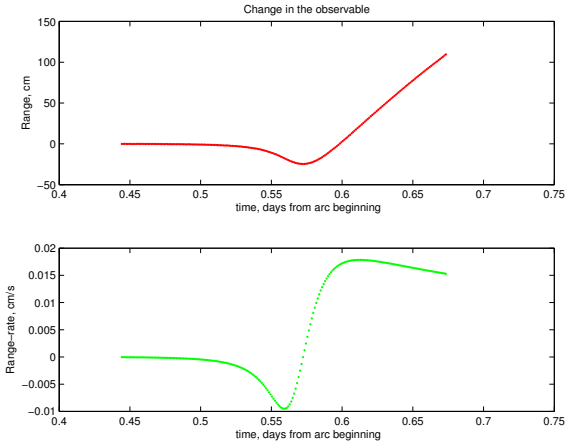

Figure 10. Sensitivity of the observables to the Lense-Thirring effect.

observe the LT precession on a planet other than the Earth was first pointed out in Iorio (2010).

In Fig. 10 we show the sensitivity of the observables to the Lense-Thirring relativistic effect (for the simulation, $GJ = 2.83 \times 10^{38}$ cm^5/s^3 has been assumed, where J is the angular momentum of Jupiter): the S/N is about 100, thus we hope to obtain a very significant constraint on the angular momentum of Jupiter.

5.3 Gravity field

One of the most important goal of the Juno mission is to accurately map the gravitational field of Jupiter with unprecedented accuracy. The very low pericenter (about 5000 km altitude) makes the orbit especially sensitive to the zonal gravity field. Through our simulation software we analyzed the impact of zonal harmonics on the observables: for example, in Fig. 11 we show the sensitivity to the degree 6 zonal harmonic C_{60} (for the simulation, $C_{60} = -3.4 \times 10^{-5}$ has been assumed). The availability of a $S/N \sim 10^5$ does not imply the possibility to solve for this individual coefficient with a relative accuracy of the order of 10^{-5}, although most

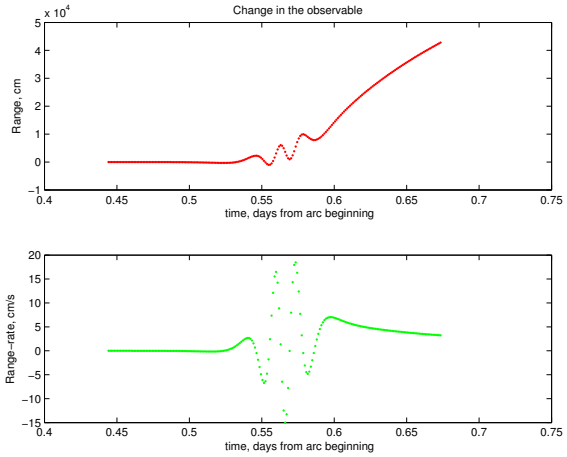

Figure 11. Sensitivity of the observables to the degree 6 zonal harmonic C_{60}.

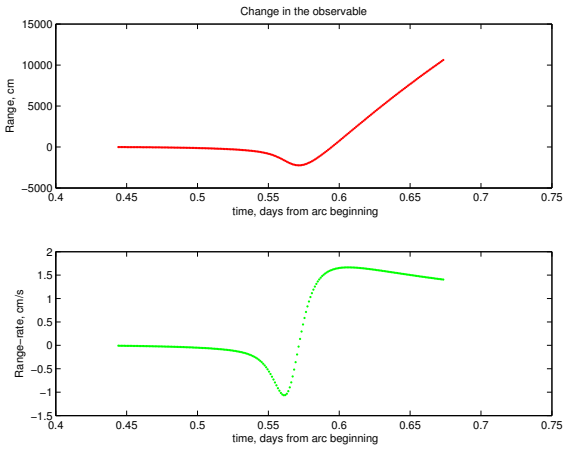

Figure 12. Sensitivity of the observables to a change of the symmetry axis by 10^{-5} radians, that is 2 arcsec.

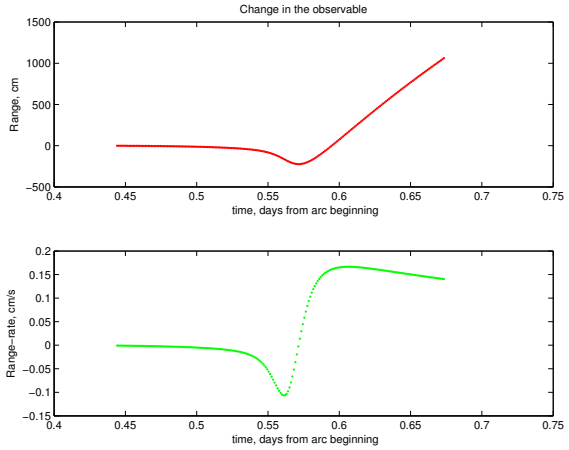

Figure 13. Sensitivity of the observables to a change of the symmetry axis by 10^{-6} radians

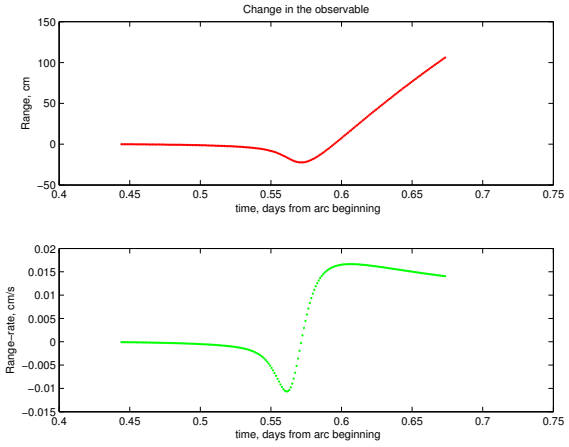

Figure 14. Sensitivity of the observables to a change of the symmetry axis by 10^{-7} radians

of the problem shows up at higher degrees (see Serra (2012)). The problems at low degrees are caused by the correlation of the zonal harmonics with the tesseral ones.

Thus, we have to take into account tesseral harmonics: look at Fig. 12, 13, 14 where we show the sensitivity of the observables to a change of the symmetry axis by 10^{-5}, 10^{-6} and 10^{-7} radians respectively. The large S/N is due to the spill into tesserals, under a small off-axis rotation, of the zonal harmonics, especially C_{20}. Thus, the accuracy in the symmetry axis is limited by the tesseral harmonics.

From Fig. 12, 13, 14 it is also clear that tesseral harmonics, even if they are small, are going to be the main source of irreducible residuals, if they are not modeled. Thus some of them will have to be solved, possibly with a priori constraints. Moreover, the zonal harmonics are strongly correlated (Kaspi et al. (2010)), thus it will be simply not possible to solve for each individual zonal harmonic beyond a comparatively low degree. E.g., for order between 24 and 30, the accuracy of the individual coefficients is going to be of the order of 10^{-4}, which is more than the expected signal. Our proposed approach is to provide a model-independent result, with reliable covariance: this could take the form of a set of gravity anomalies, limited to the well observed latitude zone, which is expected to be only 40° wide. It is possibile, using a semi-analytic theory, as done in Serra (2012), to estimate these gravity anomalies (see Fig. 15. The information about this gravity anomalies, together with the Love coefficients k_j and with the estimated angular momentum by the LT effect, should be useful to constrain models of the interior.

6 CONCLUSIONS AND FUTURE WORK

In this work, based on a preliminary but necessary analysis for the Juno RSE, we achieved a dual purpose:

1) we described the building of a simulation software, addressing the dynamical models used;
2) we showed some preparatory results about the scientific goals (gravity field of Jupiter, Love numbers and Lense-Thirring relativistic effect) using a sensitivity analysis.

The next step in the Juno RSE software development will be the implementation of a full least squares fit to the observables to solve for all the parameters of interest. As described in Sec. 2, there are different ways to do this, and we

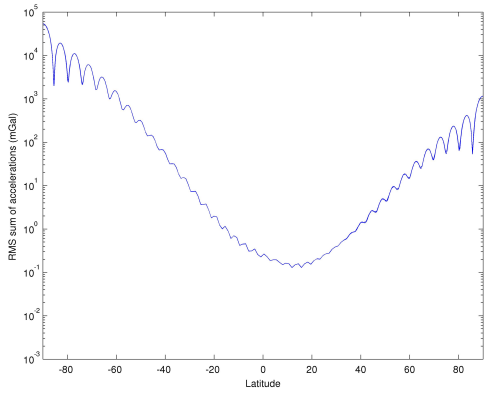

Figure 15. Gravity anomalies (semilogarithmic scale).

still have the possibility of making choices without waste of effort: the main issue to be discussed with the Juno team is whether we are supposed to use only the passes at perijove dedicated to the gravity experiment, or also other tracking sessions, to attempt a model of the intermediate arcs. Once the corrector software will be developed and tested, we will proceed to full cycle simulations of the experiment in Jupiter orbit, with the goal of pushing the performance to its intrinsic limits. This to some extent depends upon our understanding of the science goals, and from our capability of handling the mathematical difficulties of a poorly conditioned orbit determination problem.

ACKNOWLEDGMENTS

This work has been supported by the Italian Space Agency under the contract *Radioscienza per BepiColombo e Junofasi B2/C/D-Attività scientifiche* . We would like to thank the two anonymous reviewers for their suggestions.

References

E.M. Alessi, S. Cicalò, A. Milani, G. Tommei, Desaturation Maneuvers and precise orbit determination for the BepiColombo mission, Monthly Notices of Royal Astronomical Society, Volume 423, Issue 3, pp. 2270-2278 (2012)

Archinal, B. A., A'Hearn, M. F., Bowell, E., Conrad, A., Consolmagno, G. J., Courtin, R., Fukushima, T., Hestroffer, D., Hilton, J. L., Krasinsky, G. A., Neumann, G., Oberst, J., Seidelmann, P. K., Stooke, P., Tholen, D. J., Thomas, P. C., Williams, I. P., Report of the IAU Working Group on Cartographic Coordinates and Rotational Elements: 2009, Celestial Mechanics and Dynamical Astronomy, Volume 109, Issue 2, 101-135 (2011)

B. Bertotti, L. Iess, P. Tortora, A test of general relativity using radio links with the Cassini spacecraft, Nature, Volume 425, Issue 6956, 374–376 (2003)

T. Damour, M. Soffel, C. Xu, General-relativistic celestial mechanics. IV. Theory of satellite motion, Physical Review D, Volume 49, nr. 2, 618–635 (1994)

W.M. Folkner, J.G. Williams, D.H. Boggs, The Planetary and Lunar Ephemeris DE 421, JPL Memorandum IOM 343R-08-003 (2008)

L. Iess, G. Boscagli, Advanced radio science instrumentation for the mission BepiColombo to Mercury, Planetary and Space Science 49, 1597–1608 (2001)

L. Iorio, Juno, the angular momentum of Jupiter and the Lense-Thirring effect, New Astronomy, Volume 15, Issue 6, p. 554-560 (2010)

R.A. Jacobson, JUP230 - JPL satellite ephemeris (2003)

Y. Kaspi, W.B. Hubbard, A.P. Showman, G.R. Flierl, Gravitational signature of Jupiter's internal dynamics, Geophysical Research Letters, Volume 37, Issue 1, L01204 (2010)

Klioner, S.A., Capitaine, N., Folkner, W., Guinot, B., Huang, T. Y., Kopeikin, S., Petit, G., Pitjeva, E., Seidelmann, P. K., Soffel, M.: Units of Relativistic Time Scales and Associated Quantities. In: Klioner, S., Seidelmann, P.K., Soffel, M. (eds.) Relativity in Fundamental Astronomy: Dynamics, Reference Frames, and Data Analysis, IAU Symposium, 261, 79-84 (2010)

S. Matousek, The Juno New Frontiers mission, Acta Astronautica 61, 932–939 (2007)

A. Milani, G.F. Gronchi, Theory of Orbit Determination, Cambridge University Press, 2010.

A. Milani, G. Tommei, D. Vokrouhlicky, E. Latorre, S. Cicalò, Relativistic models for the BepiColombo radioscience experiment, Proceedings of the IAU Symposium 261 Relativity in Fundamental Astronomy: Dynamics, Reference Frames, and Data Analysis, Proceedings of the International Astronomical Union, IAU Symposium, Volume 261, p. 356-365 (2010)

Moyer, T.D., Formulation for Observed and Computed Values of Deep Space Network Data Types for Navigation. Wiley-Interscience (2003)

D. Serra, The Juno mission gravity science experiment, Master Degree Thesis in Mathematics, University of Pisa (2012)

Shapiro, I.I.: Fourth test of general relativity. Phys. Rev. Lett., 13, 789-791 (1964)

G. Tommei, A. Milani, D. Vokrouhlický, Light time computations for the Bepicolombo radioscience experiment, Celestial Mechanics & Dynamical Astronomy 107, 285–298 (2010)

G. Tommei, L. Dimare, A. Milani, D. Serra, Orbit determination for the radio science experiment of the NASA mission Juno, Proceedings of the IAC12, IAC-12.A3.5.4 (2012)